Multistep Closed-Loop Power Control Using Linear Receivers for DS-CDMA Systems

Lian Zhao, *Member, IEEE* and Jon W. Mark, *Life Fellow, IEEE*

Abstract—A closed-loop power control strategy, which includes both power control and power allocation functions, for a code-division multiple-access system is proposed. The target power level for a minimum mean squared error (MMSE) or a matched filter (MF) linear receiver is iteratively computed, and the power control command (PCC) is generated by comparing the received power with the generated target power. The PCC history and the channel fade slope information, which contains the Doppler effect, are used to generate variable stepsizes for regulating the transmit power level. Closed-loop power control is based on a criterion that minimizes the average transmit power and the standard deviation of the received power/signal-to-interference ratio. The power control strategy also tends to reduce the bit error rate. Simulation results demonstrate the effectiveness of the proposed power control algorithm. The results also indicate that the tracking ability of the MMSE and MF receiver is essentially similar, except that the average transmit power is lower with the MMSE receiver but is more complex to implement.

Index Terms—Adaptive stepsize, average fade slope duration, code-division multiple access (CDMA), linear receivers, power control command history, transmit power control.

I. INTRODUCTION

COMPARED to time- and frequency-division multiple access, code-division multiple access (CDMA) offers a significant capacity improvement of cellular systems [1]. However, this improvement is dependent on the effectiveness of the power control mechanism used [2], [3], especially on the uplink transmissions. Without power control, a base station (BS) would receive a much stronger signal from a mobile that is geographically closer to it than that from one that is farther away, leading to a decrease in system capacity. This is the *near–far* problem inherent in CDMA systems. Other factors that can affect system performance include path loss, shadowing, multipath fading, intracell interference, and intercell interference. The burstiness of the user traffic also has an impact on how power control should be performed. For example, a power control strategy that is suitable for persistent traffic may not be as effective for intermittent traffic. The purpose of power control is to provide a balanced counterattack to mitigate the adverse effects introduced by these factors.

Transmit power control (TPC) can be performed by using an open-loop power control and/or a closed-loop power control strategy. Open-loop control attempts to mitigate the slowly varying factors such as path loss and shadowing, while closed-loop control is used to compensate for effects due to fast fading. Open-loop is a preventive control mechanism while closed-loop is a reactive control mechanism. Reactive control is especially effective when the generation of the feedback signal captures the statistical variation of the propagation channel. Channel state information such as Doppler frequency can be derived from the observed signal at the BS receiver. With persistent transmission the feedback signal can be generated based on information extracted from the observables. In practical systems, there will be a combination of information-carrying and control signals, so that the assumption of persistent transmission is not unreasonable. An example of control signal sent by the mobile station is a vector of pilot signal strengths received from the nearby base stations for making handoff decisions in a mobile-assisted handoff scheme [4]. These control signals can be sent by piggy-backing onto the payload or as separate packets.

The frame structure of UMTS/IMT-2000 has both dedicated physical data and control channels [5]. Each frame, of 10 ms in length, is divided into 16 0.625-ms slots. In the uplink, data and control signals occupy separate slots, while in the downlink, data and control signals share the same slot. Of particular note is that the control channel has a TPC command field. With a dedicated physical control channel in both the uplink and downlink, there will always be TPC signals. The closed-loop power control method proposed in this paper, although described in the context of extracting channel state information from the observables in the uplink and generating TPC signals for the downlink, is equally applicable to extracting channel state information and generating TPC signals using the contents of the dedicated physical control channel to regulate the transmit power level by tracking the Doppler shifted channel fading gain. Thus, signaling using the dedicated control channel also represents persistent transmission. Conventional power control does not make use of the channel state information. We conjecture that the closed-loop power control strategy described in this paper should offer improved performance.

It has been shown in [6] and [7] that when the power control update frequency is much larger than the Doppler frequency, and the round-trip delay between the mobile and the BS is reasonably small, power control schemes using feedback from the BS to the mobile station (MS) can be effective in compensating for fast fading due to multipath. If the variability of the radio channel is faster than the control rate, closed-loop control is ineffective.

The conventional approach to TPC design is to use a 1-bit power control command to regulate the mobile's transmit power using a fixed stepsize. It is shown in [3] and [8] that there exists an optimal stepsize for tracking a given Doppler frequency. If the stepsize is too small, it may not be effective in compensating for the channel fading; if it is too large, it may overcompensate, thereby accentuate the power control error. In [9], a different stepsize is used for a different mobile speed, which yields an improvement over the fixed stepsize approach. An *inverse update algorithm,* where the stepsize at each iteration is made equal to the inverse of the estimated channel fade, is introduced in [6]. This algorithm offers better performance than the fixed stepsize approach at the expense of greater complexity and increased bandwidth requirements on the return channel to carry the power control stepsize in addition to the power up/down commands. All the above schemes belong to the one-step TPC regime. The shortcoming with the one-step TPC is that the power control command is discarded when an update is executed. It is conjectured that the inclusion of previous power control command bits to generate variable stepsize will enhance the tracking ability. Adaptive stepsize based on a fixed lookup table using several of the most recent power control command bits has been proposed in [10]. The shortcoming of [10] is that the stepsize selection is independent of the Doppler information.

Power control is an important resource management function [11]–[13], especially for multiclass services. Consequently, an objective of this paper is to minimize the target power and the transmit power levels through proper power allocation to the individual mobile users subject to quality of service (QoS) satisfaction. Power allocation is expected to play a more significant role in the next generation wireless communication systems, which promise to support multiple data rate and multiple QoS requirements. By employing a more advanced receiver structure such as a multiuser detector, the target power level can be reduced, leading to a lower transmit power and prolonged battery life. Minimum mean squared error (MMSE) detection [14] is based on a minimization of the mean square error between the detector output and the transmitted signal. An attractive feature of the MMSE receiver is that it can be implemented adaptively. The blind adaptive multiuser detector introduced in [15] converges to the MMSE detector without a priori knowledge of the powers and signature sequences of the interfering users. In this paper, we use an adaptive linear MMSE receiver to detect the desired signal from the received composite signal. The adaptive computational algorithm is obtained via an adaptation of the iterative computational approach described by Ulukus and Yates [16]. It is shown that the MMSE filter reduces to a matched filter (MF) when the filter coefficients are set equal to the desired signature sequence.

The focus of this paper is on the design of a closed-loop power controller to combat the effect of Rayleigh fading [3], [10]. Without loss in generality, we will assume persistent transmissions. The objective is to make the transmit power level track the channel fading gain as closely as possible, in a direction to minimize the average transmit power, the standard deviation (STD) of the received power/signal-to-interference ratio (SIR), and the bit error rate (BER). The key element in the proposed closed-loop power control is the adaptive computation of the variable stepsize for regulation of the transmit power level at the mobile station.

The salient features of the proposed closed-loop power control scheme are 1) exploitation of the power control command history and 2) stepsize adjustments based on experienced Doppler effect and fading statistics. These two features distinguish our work from that reported in the open literature. With the proposed scheme, the average power consumption, the standard deviations of the received power/SIR, and the BER are greatly reduced with only a negligible increase in computational complexity.

The remainder of this paper is organized as follows. The power control and allocation problem under consideration is stated in Section II. Section III describes the proposed closed-loop power control scheme, which includes 1) a feedforward loop to generate a sequence of 1-bit power control command, 2) a variable stepsize generator that makes use of the control command history, the Doppler information, and the channel fading statistics, and 3) a feedback loop that regulates the transmit power. Numerical results to demonstrate the effectiveness of the proposed closed-loop power control scheme are presented in Section IV, and concluding remarks are given in Section V.

II. PROBLEM STATEMENT

The objective of this paper is to derive a closed-loop power control (CLPC) strategy by minimizing the total target power for all transmitting users and by regulating the transmit power using the generated power control command (PCC) history and the rate of change of the channel fading envelope. By adaptively adjusting the transmit power to closely track the time-varying channel fading gain, the CLPC scheme also reduces the standard deviation of the received power/SIR and average transmit power. The proposed CLPC scheme is composed of three subsystems: a feedforward loop, a variable stepsize generator, and a feedback loop, as shown in Fig. 1. The feedforward loop, used to generate the target power level based on the powers and signature sequences of the transmitted signals, is located at the BS. The output from the feedforward loop is a sequence of 1-bit PCCs. The blocks C2P and P2C in the feedforward loop (Fig. 1) constitute an iterative computation of the receiver coefficients and the target power level.

The variable stepsize generator, which resides at the BS, is used to generate the stepsize $\Delta(\cdot)$. As shown in Fig. 1, the output from the feedforward loop forms one input to the variable stepsize generator; the second input is a reference stepsize vector $\mathbf{D}$, derived from the fading slope information. The output from the variable stepsize generator is the stepsize $\Delta(\cdot)$, which is transmitted to the mobile station via the downlink for transmit power control.

The feedback loop, located at the mobile station, is used to regulate the transmit power level. An attempt is made to ensure that this loop is simple to implement. The CLPC configuration shown in Fig. 1 also includes a feedback delay of an amount of kT_p s, where T_p is the power control cycle time. The uplink channel is modeled as Rayleigh fading, based on the assumption that the path loss and shadowing can be fully compensated for by using open-loop power control.

The aim is to design computational algorithms to implement 1) the C2P and P2C blocks in the feedforward loop, 2) the variable stepsize generator using PCC history and the reference
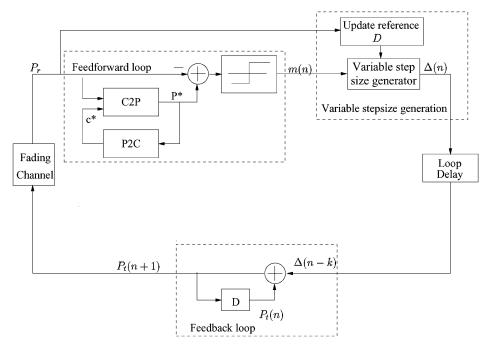
Fig. 1.   Proposed closed-loop power control model.

stepsize vector D, and 3) the generation and updating of the reference stepsize vector D.

III. Closed-Loop Power Control

As alluded to in Section II, the proposed CLPC scheme is composed of three main subsystems: a feedforward loop, a variable stepsize generator, and a feedback loop. Computational algorithms for implementing these subsystems are derived in the following subsections.

A. Feedforward Power Control Algorithm

The type of filters to implement the receiver in a direct-sequence CDMA (DS-CDMA) system has a significant impact on system performance. The optimum receiver is a maximum-likelihood multiuser detector. However, the optimum receiver is very complex to implement. Even the multistage suboptimum detector [17] is relatively complex. In this paper, we consider a conventional receiver consisting of a bank of linear MMSE filters or matched filters. An MF receiver is optimum when the received signature sequences of the multiple users are orthogonal to each other. When the orthogonality amongst the user signature sequences is destroyed by channel impairments, the MMSE receiver yields better performance than the MF receiver [14].

We consider an asynchronous BPSK-CDMA system where users transmit independent of other users. The ith user is allocated a unique signature sequence $\mathbf{s}_i$, which is an N-dimensional column vector. The QoS is SIR, with specification γ^* corresponding to a target BER*. In a time-varying environment, the instantaneous signal-to-interference ratio is a random variable; the average signal-to-interference ratio is a better QoS measure. For notational simplicity, we will use SIR to represent average signal-to-interference ratio in the sequel. Satisfactory QoS performance requires that SIR$\geq \gamma^*$. The composite received signal $r(t)$ is sampled at the chip rate. The ith discrete-time filter attempts to coherently extract the ith transmitted signal and in-

coherently detect the signals from other transmitters. By coherent and incoherent detection, it is meant that the ith filter sees the signature sequence $\mathbf{s}_i$ in its entirety, representing a whole data symbol, but only has partial observations of other transmitted signature sequences belonging to two adjacent symbols. Let $\hat{\mathbf{s}}_j, j \neq i$, represent a concatenation of elements of $\mathbf{s}_j$ belonging to two adjacent symbols of the jth transmitted signal. As seen by the ith discrete-time filter, the received signal can be represented as

$$\mathbf{r} = \sqrt{p_i} b_i \mathbf{s}_i + \sum_{j=1, j \neq i}^{K} \sqrt{p_j} b_j \hat{\mathbf{s}}_j + \mathbf{u} \qquad (1)$$

where K is the number of users in the system, and b_j and p_j are, respectively, the information bit and the received power. The term $\mathbf{u} = (u_1, \ldots, u_N)^t$ is an N-dimensional white Gaussian noise vector with per-component zero-mean and variance $E[u_l^2] = \sigma_n^2$, where the superscript t denotes matrix transpose. Let $\mathbf{c}_i$ be the N-dimensional column vector representing the coefficients of the ith MMSE filter. The ith filter output is given by

$$
\begin{aligned}
y_i &= \mathbf{c}_i^t \mathbf{r} \\
&= \sqrt{p_i} b_i \left(\mathbf{c}_i^t \mathbf{s}_i \right) + \sum_{j=1, j \neq i}^{K} \sqrt{p_j} b_j \left(\mathbf{c}_i^t \hat{\mathbf{s}}_j \right) + n_i \qquad (2)
\end{aligned}
$$

where $n_i = \mathbf{c}_i^t \mathbf{u}$ is a Gaussian random variable with zero mean and variance $\sigma_n^2 \mathbf{c}_i^t \mathbf{c}_i$ and the superscript t denotes matrix transpose. The SIR at the output of the ith receive filter is given by

$$\text{SIR}_i = \frac{p_i \left(\mathbf{c_i^t s_i} \right)^2}{\left(\mathbf{c_i^t c_i} \right) \sigma_n^2 + \sum_{j \neq i} p_j \left(\mathbf{c_i^t \hat{s}_j} \right)^2}. \qquad (3)$$

Our aim is to find the optimal target powers $\mathbf{p}^* = [p_1^*, p_2^*, \ldots, p_K^*]$ and filter coefficients $\mathbf{c}_i$ for $i = 1, \ldots, K$,

such that the total power is minimized subject to the constraint $\text{SIR}_i \geq \gamma_i^*$. The problem can be mathematically stated as

$$\min \sum_{i=1}^{K} p_i^* \tag{4}$$

$$\text{such that } p_i^* \geq \gamma_i^* \frac{\sum_{j \neq i} p_j \left(\mathbf{c_i^t \hat{s}_j}\right)^2 + \left(\mathbf{c_i^t c_i}\right) \sigma_n^2}{\left(\mathbf{c_i^t s_i}\right)^2} \tag{5}$$

$$p_i^* > 0, \quad \mathbf{c}_i \in \mathbf{R}^N. \tag{6}$$

The goal is to establish a computational algorithm to compute the filter coefficients and then the target power levels iteratively. To this end, define

$$I_i(\mathbf{p}^*, \mathbf{c}_i) = \gamma_i^* \frac{\sum_{j \neq i} p_j \left(\mathbf{c}_i^t \hat{\mathbf{s}}_j\right)^2 + \left(\mathbf{c}_i^t \mathbf{c}_i\right) \sigma_n^2}{\left(\mathbf{c}_i^t \mathbf{s}_i\right)^2} \tag{7}$$

and

$$T_i(\mathbf{p}^*) = \min_{\mathbf{c}_i} I_i(\mathbf{p}^*, \mathbf{c}_i). \tag{8}$$

The target power at the $(n+1)$th iteration can be written as

$$\mathbf{p}^*(n+1) = \mathbf{T}(\mathbf{p}^*(n)) \tag{9}$$

where

$$\mathbf{T}(\mathbf{p}^*) = [T_1(\mathbf{p}^*), \ldots, T_K(\mathbf{p}^*)]^t. \tag{10}$$

The convergence of the iterative algorithm of the form (9) has been shown in [16], [18], and [20]. An iterative algorithm for the ith filter can be written as [16]

$$\begin{aligned} &\mathbf{c}_i(n) \\ &= \sqrt{p_i} \left(1 + p_i \mathbf{s}_i^t \mathbf{A}_i^{-1}(\mathbf{p}^*(n)) \mathbf{s}_i\right)^{-1} \mathbf{A}_i^{-1}(\mathbf{p}^*(n)) \mathbf{s}_i \end{aligned} \tag{11}$$

$$\begin{aligned} &p_i^*(n+1) \\ &= \gamma_i^* \left[\frac{\sum_{j \neq i} p_j \left(\mathbf{c}_i^t(n) \hat{\mathbf{s}}_j\right)^2 + \left(\mathbf{c}_i^t(n) \mathbf{c}_i(n)\right) \sigma_n^2}{\left(\mathbf{c}_i^t(n) \mathbf{s}_i\right)^2} \right] \end{aligned} \tag{12}$$

where the $N \times N$ matrix $\mathbf{A}$ is a function of the powers and signature sequences of the interferers, given by

$$\mathbf{A}_i = \sum_{j \neq i} p_j \hat{\mathbf{s}}_j \hat{\mathbf{s}}_j^t + \sigma_n^2 \mathbf{I} \tag{13}$$

and $\mathbf{I}$ is an identity matrix.

Let $P_t^i(n)$ be the transmit power of, and $P_r^i(n)$ be the received power from, the ith user at the nth time instant. The received and transmitted powers in dB are related by

$$P_r^i(n) = P_t^i(n) + Z^i(n) \tag{14}$$

where $Z^i(n) = 20 \log_{10} z^i(n)$ is the fading gain in dB and $z^i(n)$ is the fading amplitude at time instant n. The received signal power $P_r^i(n)$ and the MMSE filter coefficients $\mathbf{c}_i(n)$ are used to generate the desired power level $P^*(n+1)$ by the functional block C2P, which is an implementation of (12). Then, the desired power level $P^*(n+1)$ is fed back to the functional block

P2C using (11) to update the filter coefficients $\mathbf{c}_i(n+1)$, which are used in the next power control cycle to update the target power. The received power $P_r^i(n)$ is then compared with the desired power level $P^*(n)$ to generate a PCC bit, which is fed to the variable stepsize generation subsystem. For the conventional MF receiver, the P2C block is removed, and the signature sequence is used for despreading, i.e., $\mathbf{c}_i = \mathbf{s}_i$. In the following, we will omit the superscript i in (14) for notational simplicity.

B. Feedback Power Control Algorithm

As shown in Fig. 1, the feedback control loop, which resides at the mobile station, regulates the transmit power by adding the received stepsize $\Delta(\cdot)$ transmitted from the BS controller to the current transmit power level. In this way, the MS's role in performing closed-loop power control is relatively simple.

Let T_p be the power control cycle time. The transmit power is updated at the start of each power control cycle. Let n be the time index in units of T_p, $P_t(n)$ be the transmit power at the end of the nth power control cycle, and $\Delta(n)$ be the stepsize generated by the variable stepsize generator at time instant n at the base station and sent to the mobile station via the downlink. The transmit power level at time instant $n+1$ is given by

$$P_t(n+1) = P_t(n) + \Delta(n-k) \tag{15}$$

where k is the loop delay index, in units of T_p.

C. Generation of Variable Stepsize, $\Delta(n)$

As indicated in (15), the key to the success of TPC is the generation of the stepsize $\Delta(\cdot)$. The objective in generating the variable stepsize $\Delta(\cdot)$ is to regulate the transmit power level to track the trajectory of the Rayleigh fading gain. The slope of the fading envelope is a function of the Doppler frequency or the mobile speed. For a given minimum-to-maximum excursion of the fading envelope, i.e., a positive-going fading envelope segment, we can construct a set of stepsize $\delta(\cdot)$, as illustrated in Fig. 2, and form a reference stepsize vector

$$D = [\delta(1) \, \delta(2) \ldots \delta(L)]^t \tag{16}$$

obtained by averaging over a number of positive-going slopes. The index L is the maximum number of steps in a positive-going slope used to construct the reference stepsize vector. As discussed in Section III-C1, the reference stepsize vector for a given mobile speed or Doppler frequency is generated by averaging over W consecutive positive-going slopes.

Let

$$\mathbf{m} = [m(n) \, m(n-1) \, \ldots \, m(n-L)]^t \tag{17}$$

be the PCC bit vector, where $m(n)$ is the most recent PCC bit generated at time instant n, obtained by comparing the received power $P_r(n)$ with the generated target level $P^*(n)$. For one-step power control, only the command bit $m(n)$ is used for transmit power updating; while for the proposed multistep adaptive power control, the contents from $m(n)$ down to $m(n-L)$
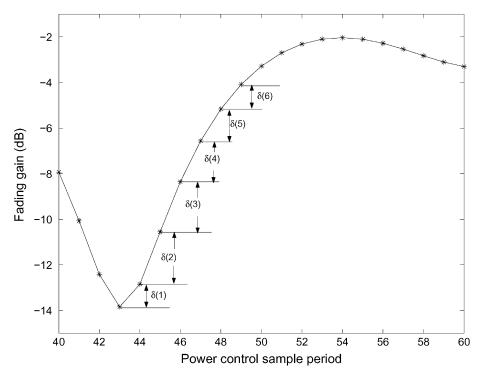
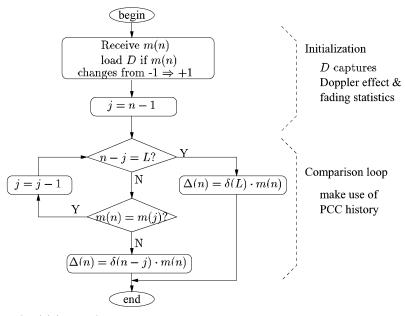Fig. 2. Illustration of the reference stepsize generation.

Fig. 3. Flowchart for adaptive stepsize $\Delta(n)$ generation.

are used to generate the applied stepsize. The length L is also called the PCC memory length.

The length of the PCC count of consecutive $+1$s or -1s is then used to select the appropriate $\delta(\cdot)$ as the stepsize $\Delta(n)$ at the nth time instant. The generation of $\Delta(n)$ by updating the reference vector and by using the PCC counts to select the appropriate $\delta(\cdot)$ is shown in the flowchart of Fig. 3. The process includes two steps: an initialization phase and a comparison loop. The initialization includes inputting the reference stepsize vector D and updating when the PCC bit $m(n)$ changes from -1 to $+1$. The purpose of this step is to make the applied stepsize $\Delta(n)$ to relate to the Doppler effect and fading statistics. Inside the comparison loop, the received $m(n)$ is compared with the previous PCC bits.

The first test to terminate the loop is to check the memory length L. When the memory length is reached, the assigned stepsize is $\Delta(n) = \delta(L) \cdot m(n)$. The second test to terminate the loop is when an opposite PCC bit is encountered before reaching the memory size L. Then the assigned stepsize is $\Delta(n) = \delta(n-j) \cdot m(n)$, where $(n-j)$ denotes number of comparisons made when an opposite PCC is reached. It is noted that all the elements in D are positive; therefore, the sign of $\Delta(n)$ is specified by $m(n)$, i.e., multiplying $\delta(\cdot)$ with $m(n)$ to take the proper sign. The purpose of this loop is to relate the generation of $\Delta(n)$ to the PCC history in an attempt to track the fading process.

The stepsize $\Delta(n)$ is thus a function of the reference stepsize vector D and the PCC history. The construction of the reference

stepsize vector captures the fading slope information, while the counting of the PCC bits provides a pointer to select the appropriate component of the vector D.

1) Generation of Reference Stepsize Vector: The reference stepsizes $\delta(1)$ to $\delta(L)$ are obtained by taking statistical average over the fading slopes. Fig. 2 shows a typical fading process varying from a valley to a peak. By recording the stepsizes in each positive-going fading slope, we can generate a reference stepsize vector $D_i = [\delta_i(1)\ \delta_i(2)\ldots\delta_i(L)]^t, i = 1,\ldots,W$, where W is the number of positive-going slopes used to generate the reference stepsize vector D. A sample of W consecutive positive-going slope stepsizes is shown in the following matrix:

$$
\begin{bmatrix}
\delta_1(1) & \delta_2(1) & \cdots & \delta_W(1) \\
\delta_1(2) & \delta_2(2) & \cdots & \delta_W(2) \\
\vdots & \vdots & \vdots & \vdots \\
\delta_1(L) & \delta_2(L) & \cdots & \delta_W(L)
\end{bmatrix}
\tag{18}
$$

where each column is the fading stepsizes of a positive-going slope. For slopes where the step length l is less than L, zeroes are used to fill in the rows from $(l+1)$ to L of the corresponding columns. When $l > L$, the stepsizes beyond L are discarded. The elements in D are obtained by averaging over the rows of the nonzero elements

$$
\delta(j) = \frac{1}{W_j} \sum_{i=1}^{W} \delta_i(j)
\tag{19}
$$

where W_j is the number of nonzero elements in the jth row of matrix (18). Consequently, $\delta(1)$ is the average of the fading gain difference between the lowest fade and the second lowest fade, and so on. This procedure takes place once when the PCC changes from -1 to $+1$, i.e., a new column is written into the rightmost of (18), while the leftmost column is dropped. When the vector D is updated, the matrix shifts one column to the left, leaving the rightmost column for writing in the new fading slope data.

The initialization of the matrix can be implemented by using a unit matrix, i.e., with all the elements being $+1$ at the beginning. This is equivalent to the conventional fixed stepsize power control. The matrix will reflect the practical fading slope information after a short transient period. If a training sequence is applied, the steady state of the adaptation can be obtained without the transient period.

In the following, we will analyze the statistics of a single ray Rayleigh fading case, and will show that the expected value of the stepsize is a function of the normalized Doppler frequency f_dT_p, where f_d is the Doppler frequency and, as defined earlier, T_p is the power control cycle. Consequently, the Doppler information and fading statistics are embedded in the reference stepsize vector D.

2) Fading Process Reconstruction: For the updating of the reference stepsize vector D, fading process reconstruction is required. Since the received signal power of the desired user needs to be measured in each power control cycle, we can use this information to construct the experienced fading process.
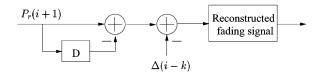

Fig. 4. Structure of fading process reconstruction.

Fig. 4 shows the procedures to reconstruct the fading process. The received powers for two adjacent power control cycles are

$$
\begin{aligned}
P_r(i+1) &= P_t(i+1) + Z(i+1) \\
&= P_t(i) + \Delta(i-k) + Z(i+1)
\end{aligned}
\tag{20}
$$
$$
P_r(i) = P_t(i) + Z(i).
\tag{21}
$$

The power difference is thus

$$
P_r(i+1) - P_r(i) = Z(i+1) - Z(i) + \Delta(i-k)
\tag{22}
$$

which yields the fading gain difference for the adjacent samples, with bias $\Delta(i-k)$. At the beginning of the construction, the reference level can be selected to be zero or any other meaningful value.

Using the fading process reconstruction shown in Fig. 4, (18) can be updated online. The averages from (18) are sent to the variable stepsize generator to generate the stepsize $\Delta(n)$. The advantage of the proposed approach is that the variation of the Doppler frequency and fading statistics can be captured in "real time" using the existing power control algorithm.

3) Selection of Memory Length L: In order to provide a reference to select the memory length L, we define the *average fade slope duration* (AFSD) as the average number of sampling steps during an interval when the envelope transits from a local minimum to a local maximum. In what follows, we introduce an approximate analysis to determine the AFSD. A more accurate analysis is described in [22].

Let a and b be a pair of adjacent maximum and minimum points of the Rayleigh envelope function, and V be the fading stepsize between the adjacent samples. Then the *fade slope duration* is defined as

$$
L_f = \frac{a - b}{V}.
\tag{23}
$$

Let $\dot{z}(t)$ be the slope of the fading envelope $z(t)$ at time instant t. Assume that the diffuse component of the received bandpass signal is symmetrical about the carrier frequency. The probability density function (pdf) of $\dot{z}$ follows a Gaussian distribution with zero mean and variance $\sigma_s^2 = 2(\pi f_d \sigma)^2$ [21], where $2\sigma^2$ is the average fading power

$$
p(\dot{z}) = \frac{1}{\sqrt{2\pi}\sigma_s} \exp\left(\frac{-\dot{z}^2}{2\sigma_s^2}\right).
\tag{24}
$$

The mean for the stepsize V is given by

$$
\begin{aligned}
E[V] &= E[\dot{z}_+] \cdot T_p = T_p \int_0^\infty \dot{z} \cdot \frac{2}{\sqrt{2\pi}\sigma_s} \exp\left(-\frac{\dot{z}^2}{2\sigma_s^2}\right) d\dot{z} \\
&= 2\sqrt{\pi}\sigma f_d T_p
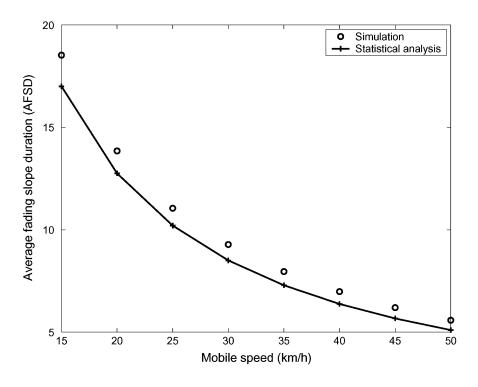\end{aligned}
\tag{25}
$$

Fig. 5.   AFSD as a function of the mobile speed.

where $E[\dot{z}_+]$ denotes the expectation of the positive slope. Taking expectation on both sides of (23), the AFSD is approximately given by

$$E[L_f] = \frac{E[a] - E[b]}{E[V]}. \tag{26}$$

Strictly speaking, $E[a]$ ($E[b]$) should be the ensemble average of maxima (minima). However, analytical derivation of $E[a]$ is difficult. To facilitate analytical assessment, we define a statistical maximum (minimum) as per Proposition 1 [22].

Proposition 1: The statistical maximum $E[a]$ (minimum, $E[b]$) is given by the area of the envelope function above (below) the median (or mean).

Proposition 1 is a statistical characterization of the maxima and minima of the envelope function. With a Rayleigh distributed envelope, the median m_z, which is defined as the point at which $\Pr(z < m_z) = \Pr(z > m_z) = 1/2$, is $m_z = \sqrt{2\ln 2}\sigma$. The mean values of the envelope below and above m_z are given by

$$E[b] = \int_0^{m_z} z \cdot \frac{2z}{\sigma^2} \exp\left(-\frac{z^2}{2\sigma^2}\right) dz$$
$$= -2m_z \exp\left(-\frac{m_z^2}{2\sigma^2}\right) + 2\sqrt{2\pi}\sigma \left[\frac{1}{2} - Q\left(\frac{m_z}{\sigma}\right)\right] \tag{27}$$

and

$$E[a] = \int_{m_z}^{\infty} z \cdot \frac{2z}{\sigma^2} \exp\left(-\frac{z^2}{2\sigma^2}\right) dz$$
$$= 2m_z \exp\left(-\frac{m_z^2}{2\sigma^2}\right) + 2\sqrt{2\pi}\sigma Q\left(\frac{m_z}{\sigma}\right) \tag{28}$$

where $Q(x)$ is the complementary cumulative distribution function of the standard normal distribution. By substituting the above values for $E[a], E[b], E[V]$, and m_z into (26), we obtain

$$E[L_f] = \frac{E[b] - E[a]}{E[V]}$$
$$= \frac{1}{\sqrt{\pi}f_d T_p}\{\sqrt{2\ln 2} + \sqrt{2\pi}[2Q(\sqrt{2\ln 2}) - 1/2]\}$$
$$= 0.2952/f_d T_p. \tag{29}$$

Fig. 5 shows the simulated AFSD and the approximate analytical AFSD given in (29) for various mobile speeds. We note in passing that using the more accurate analysis of AFSD from [22], the analytical and simulation results coincide. For all the numerical results reported in this paper, the carrier frequency is assumed to be 2 GHz, and power control interval is $T_p = 0.625$ ms, which is equivalent to a power control frequency of 1600 Hz. [1] The PCC memory length L is selected based on the L_f values. We note from the stepsize generation procedure that the stepsize difference becomes smaller when the index is larger than six. Thus, we set the maximum memory length to nine for the range of mobile speeds considered in Section IV.

4) Selection of Window Length W: The window length W is determined by the memory size and fading correlation. If W is too large, it brings hysteresis in response to the variations of the Doppler frequency and fading statistics. If W is too small, the vector D cannot capture the average effect of the fading. In the simulation, we select $W = 100$. This is based on the simulation results that for a given Doppler frequency, when $W > 100$, the reference stepsize vector does not change significantly.

---

[1]This is the power control frequency specification in IMT-2000 W-CDMA [23].
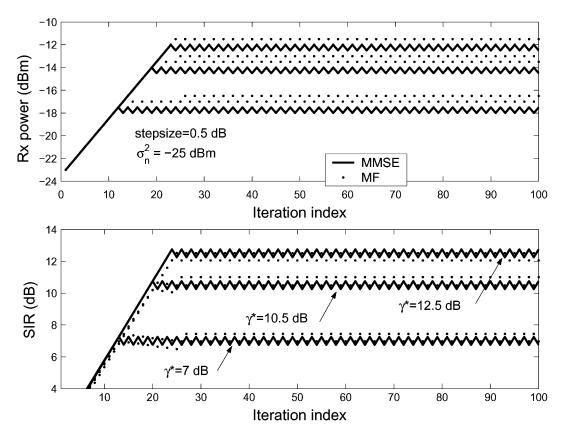
Fig. 6. Received power and SIR for the MMSE/MF iteration algorithm with up/down feedback (stepsize $= 0, 5$ dB, no fading).

IV. NUMERICAL RESULTS

In this section, simulation results are presented to illustrate the effectiveness of the proposed CLPC algorithm. In the following, the results for the conventional one-step fixed stepsize power control are first presented to gain a basic idea of TPC and also to set a benchmark for the performance of the proposed multistep adaptive stepsize TPC. TPC performance is analyzed in terms of the STD of the received power/SIR, average transmit power, and average BER. The numerical results presented in this section have been obtained by simulating 20 000 power control cycles.

A. Conventional Fixed Stepsize TPC

Fig. 6 shows the received power and the corresponding SIR for the case without fading using a 0.5 dB stepsize. In the numerical study the system supports three classes of service, with target $\gamma^* = \{7, 10.5, 12.5\}$ dB, and the number of users $\{10, 5, 5\}$, respectively. Each user is allocated a Gold sequence with length 31. The polynomials for the Gold sequence are 24 and 35 in octal notation. For simplicity, data rate is assumed to be the same across all classes. Furthermore, the additive white Gaussian noise (AWGN) power level is $\sigma_n^2 = 10^{-5.5}$ W (-25 dBm). At the beginning of the iterations, the transmit power is set at -23 dBm, and the filter coefficients are initialized to be the signature sequences of the users. It can be seen that the power converges after 20–30 iterations. With a larger stepsize, the convergence is faster but with larger fluctuations. The corresponding results for the conventional MF receiver, i.e., without filter coefficients updating, are given by the dotted

curves. It shows that the target power level of the MF receiver is higher than that of the MMSE receiver.

Fig. 7 is an illustration of the fixed stepsize power control, where the target power level is determined by the forward loop power control. Here, each user experiences fading independent of other users' fading. The desired user has a target γ^* of 7 dB. The other parameter values used are $f_d T_p = 0.0116$ ($v = 10$ km/h), power control stepsize equals 1.25 dB, which is the best value for this mobile speed, with no transmission delay. Under these conditions, we can see that the conventional CLPC with fixed stepsize of 1.25 dB works quite well. The received power STD is reduced to 1.494 dB.

We also simulated the received power STD as a function of the stepsize. The simulation stepsize changes from 0.25 to 2 dB with a 0.25 dB increment. The best stepsizes to minimize the received power STD are [1.0, 1.25, 1.25, 1.5, 1.5, 1.5, 1.5, 1.5, 1.5, 0.75] dB for mobile speed varying from 5 to 50 km/h with 5 km/h increment.

In a cellular system, there is own cell interference, other cell interference, and background noise. Other cell interference may be modeled as similar to own cell interference or background noise, when the number of interferers are large. If other cell interference were modeled as a fraction of own cell interference, then the total interference (own cell plus other cell) would be increased by a fraction f. This would mean that, to maintain the same capacity at the same target BER, the target signal power would have to be proportionally increased. If other cell interference were modeled as similar to background noise, then the total additive noise level would be increased.
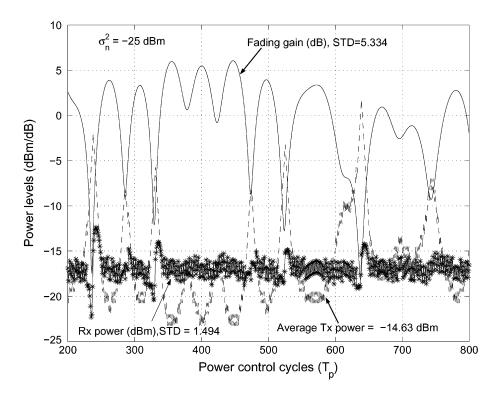
Fig. 7. Fixed stepsize power control (noise power $\sigma_n^2 = -25$ dBm, $f_d T_p = 0.0116$ ($v = 10$ km/h), no feedback delay, stepsize $= 1.25$ dB).
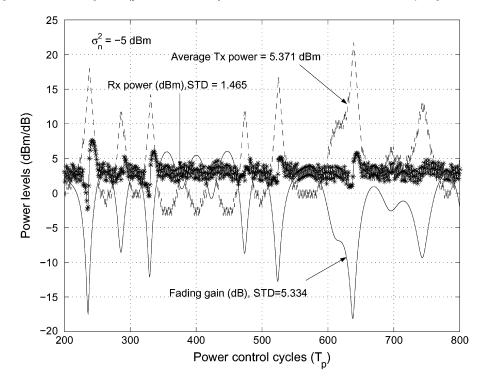

Fig. 8. Fixed stepsize power control (background noise power $\sigma_n^2 = -5$ dBm, $f_d T_p = 0.0116$ ($v = 10$ km/h), no feedback delay, stepsize $= 1.25$ dB).

Fig. 8 shows the scenario in which the total noise power is increased from -25 dBm (in Fig. 7) to -5 dBm. Comparing Figs. 7 and 8, it is observed that, except for a rigid shift in the transmitted and received power levels, the standard deviation of the received power is approximately the same.

It is conjectured that other cell interference has the effect of increasing the target signal power, to maintain the system capacity at the same target BER, if the interference is modeled as similar to own cell interference, or an increase in the background noise level. In either case, the tracking ability of the proposed CLPC is not affected.

B. Multistep Adaptive Stepsize TPC

Figs. 9(a) and (b) and 10(a) and (b) show a snapshot of the tracking ability of the adaptive stepsize and fixed stepsize TPC, respectively, for 100 power control cycles with $f_d T_p = 0.046$
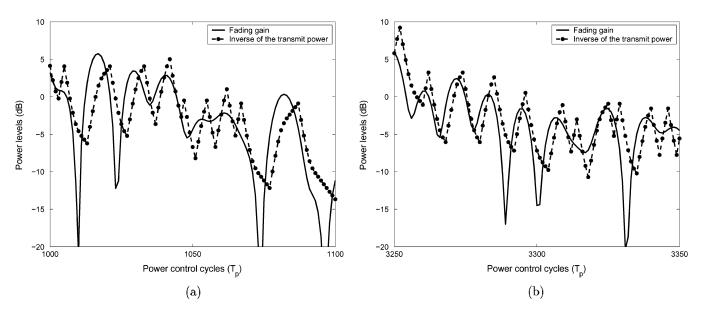
Fig. 9.   Tracking capability of adaptive stepsize power control (with $f_d T_p = 0.0463$ ($v = 40$ km/h), $2T_p$ feedback delay). (a) Profile 1 and (b) Profile 2.
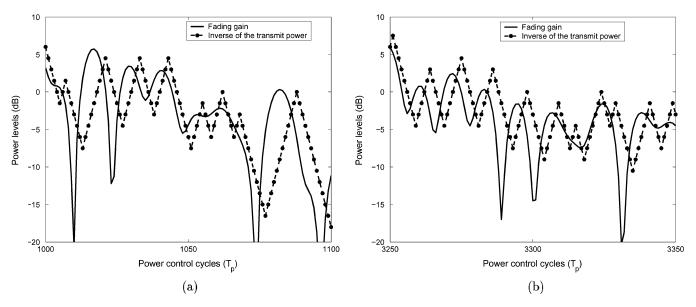

Fig. 10.   Tracking capability of fixed stepsize power control (with $f_d T_p = 0.0463$ ($v = 40$ km/h), $2T_p$ feedback delay, stepsize $= 1.5$ dB). (a) Profile 1 and (b) Profile 2.

($v = 40$ km/h) and $2T_p$ loop delay. In the figures, the transmit power is upshifted (aimed for 0 dB target received power) and reversed $(-P_t)$ in order to have a good visual effect.

It is observed that adaptive stepsize TPC attempts to use curves to fit the variations of the fading gain. The fixed stepsize TPC uses straight lines; in most cases, the straight lines go beyond the fading gain in both directions, which implies that transmit power is reduced too low or is increased too high, because of the loop delay. On the other hand, when the fading gain goes from the peaks to the valleys, for adaptive stepsize TPC, a seemingly reasonable solution is that the stepsizes should be changed from smaller stepsizes to larger stepsizes (inverse when the fading is up). Without loop delay, this approach would be desirable to make the transmit power well fit the fading variation. In the presence of loop delay, this kind of stepsize allocation scheme will lead to a poor tracking performance. When executing a "+1" power control command,

the use of a large positive $\delta(1)$ (shown in the figures as the first down steps) can actually compensate for some loop delay. Simulation results show that, in most cases, better tracking ability can be achieved when the stepsize is set symmetric for power up/down commands.

Next, we present simulation performance measures of the TPC algorithms. For simplicity, we model a fixed Doppler frequency in each simulation run. Table I lists the received power STD for the fixed stepsize TPC, the adaptive stepsize TPC, and the percentage gain of the adaptive over the fixed stepsize TPC by using the MMSE receiver. It can be seen that the percentage gain increases almost monotonically with the increase of the normalized Doppler frequency in the range of interest. The gain exceeds 10% when the normalized Doppler frequency $f_d T_p$ is higher than 0.0347.

Fig. 11 shows the STD of the received power by using MMSE/MF receivers and adaptive/fixed stepsize TPC. The

TABLE I
RECEIVED POWER STD (dB) WITH DIFFERENT STEPSIZE SELECTION AND THE PERCENTAGE GAIN IN STD REDUCTION

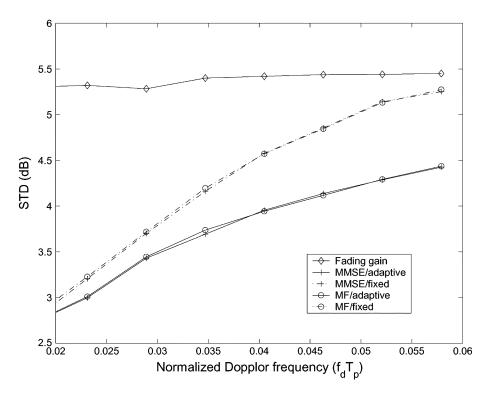| Speed(km/h)	20	25	30	35	40	45	50
$f_d T_p$ (10^{-2})	2.31	2.89	3.47	4.05	4.63	5.21	5.79
Fixed stepsize (dB)	3.205	3.701	4.161	4.576	4.854	5.141	5.251
Adap. stepsize (dB)	2.997	3.430	3.692	3.955	4.137	4.287	4.426
Percent. improvement	6.51	7.33	11.25	13.59	14.76	16.60	15.72

Fig. 11. Received power STD for adaptive stepsize and fixed stepsize power control with MMSE and MF receivers.

curves from the top to the bottom are the STD of the fading gain, fixed stepsize TPC, and adaptive stepsize TPC for the MF and MMSE receivers, respectively. It is noted that the received power STD monotonically increases with $f_d T_p$. There is a negligible difference for MF and MMSE receivers in terms of the tracking ability. It is shown that significant improvement can be attained by using the proposed adaptive stepsize power control, especially when the normalized Doppler frequency is high.

Fig. 12 shows the average transmit power versus the normalized Doppler frequency. The upper four curves are the results for the user with $\gamma^* = 12.5$ dB, and the lower four curves are for $\gamma^* = 7$ dB. It is observed that, over a wide range of $f_d T_p$ values, the MF receiver requires a higher transmit power compared to the MMSE receiver, and the average transmit power is lower for adaptive TPC compared to fixed TPC. From Fig. 6, the target power is about -18 and -12 dBm for $\gamma^* = 7$ dB and $\gamma^* = 12.5$ dB, respectively. Although the average fading power is assumed as "1" in the simulation, extra power is required to smooth out the fading effect. It is also observed that the average transmit power decreases as the normalized Doppler frequency increases. This trend implies that a higher transmit power is required in order to achieve better tracking. This is intuitively cor-

rect. For perfect tracking, i.e., the received power is a constant, the required transmit power is infinity. For no TPC, i.e., no attempt to track, the average transmit power is the target power. From Fig. 12, it is observed that, for both the MF and MMSE receivers, the slope of fixed TPC is steeper than that of adaptive TPC. Based on the above analysis, it is conjectured that a steeper slope implies that, in the fixed TPC case, the tracking ability will deteriorate faster when the Doppler frequency becomes larger.

In the simulation, the instantaneous SIR is obtained by using (3) in each power control cycle. Fig. 13(a) and (b) shows the pdf of the SIR when $f_d T_p = 0.0231$ ($v = 20$ km/h) and $f_d T_p = 0.0462$ ($v = 40$ km/h), representing a low speed and a medium speed, respectively, for adaptive stepsize TPC (solid curves) and fixed stepsize TPC (square dashed curves). It can be seen that adaptive stepsize TPC distributes the received SIR about the neighborhood of γ^* (10.5 dB) with a higher probability, i.e., a smaller STD.

Fig. 14 shows the BER obtained by averaging the SIR within the neighborhood of $\pm 1.5\sigma_\gamma$ of the γ^*, where σ_γ denotes the STD of the received SIR in dB. The purpose of this truncation is to eliminate the affect of the tails of the SIR distribution on the average BER. Fig. 14(a)–(c) shows the average BER for the
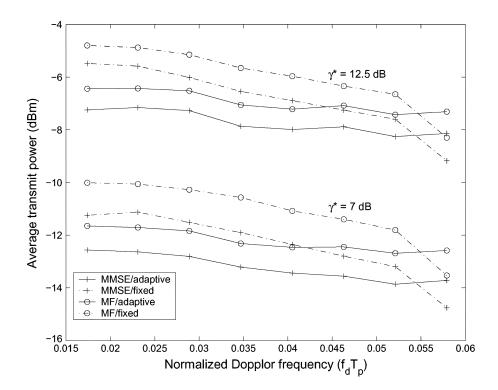
Fig. 12.   Average transmit power for adaptive stepsize and fixed stepsize power control with MMSE and MF receivers.
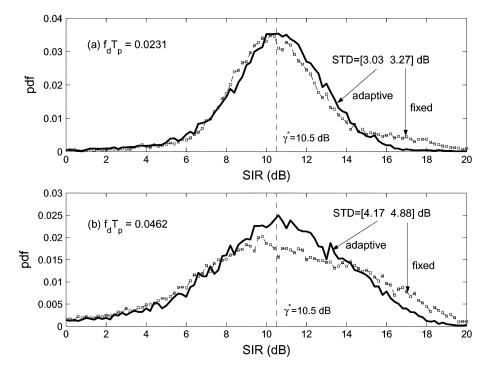

Fig. 13.   PDF of the received SIR for adaptive stepsize and fixed stepsize power control with MMSE receiver ($\gamma^* = 10.5$ dB).

users with target SIR at 7, 10.5, and 12.5 dB, respectively. It is observed that, as the Doppler frequency increases, the BER performance degrades. The rate of degradation is faster for the fixed stepsize TPC, because of its poorer tracking ability.

Fig. 15 shows the BER performance when the target γ^* varies from 2 to 20 dB. The curves in this figure have been obtained by simulating a system supporting ten users, where the desired user changes its γ^*, and the other users' γ^* is fixed at 7 dB, with $f_d T_p = 0.0462$ and $2T_p$ loop delay. The upper and lower triangle curves are the results for flat Rayleigh fading without TPC and the results for AWGN channel, respectively. Again, the BER performance difference for the MMSE and MF receivers is negligible. By using adaptive stepsize TPC, the BER curve shifts closer to that of AWGN. The target SIR reduction is about 1 dB for adaptive over fixed TPC.

Table II lists the average transmit power and the power reduction by using adaptive and fixed stepsize TPC with MMSE and MF receivers. The simulation environment is nearly the same as
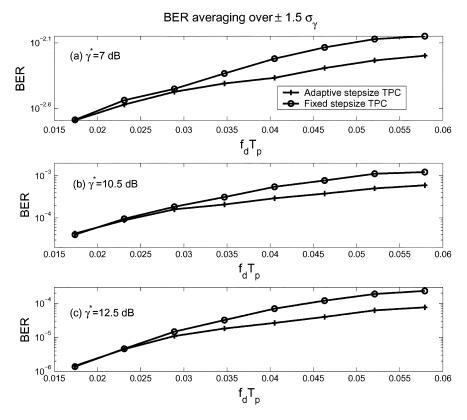
Fig. 14.   BER versus normalized Doppler frequency ($\pm 1.5\sigma_\gamma$ neighborhood of the γ^* averaging).
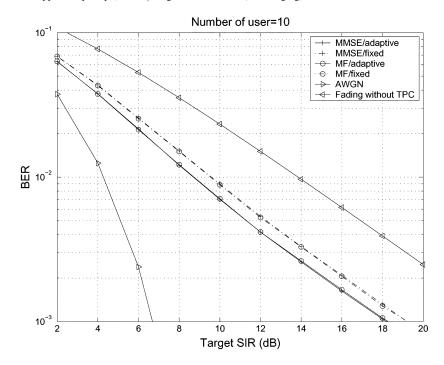

Fig. 15.   BER versus target SIR ($f_d T_p = 0.0462$, $2T_p$ delay).

that in Fig. 15, i.e., the target SIR for the desired user changes from 2 to 20 dB, and the target SIR for the interferers is fixed at 7 dB. The three groups denote the results for the number of users being 10, 20, and 28,[2] denoting the light-load, medium-load, and high-load cases, respectively. Inside each group, the first

two rows are the average transmit power using MMSE and MF receivers, and the third row is the power reduction (with italic numbers) by using the MMSE over the MF receiver for adaptive TPC. The remaining three rows list similar results for fixed TPC. Our results show that with the increase in the number of users, the power savings by using the MMSE receiver is more significant. When the number of users is relatively low, it is more

[2]With a Gold sequence of length 31, this is about the largest number of users that can be supported.

TABLE II
AVERAGE TRANSMIT POWERS (dBm) AND POWER REDUCTION (dB) BY USING MMSE OVER MF RECEIVER ($f_d T_p = 0.0462$, $2T_p$ LOOP DELAY)

K=10/20/28	2	4	6	8	10	12	14	16	18	20
MMSE/adap.	-18.63	-16.66	-14.68	-12.68	-10.65	-8.68	-6.68	-4.67	-2.66	-0.68
MF/adap.	-18.42	-16.39	-14.41	-12.47	-10.45	-8.46	-6.44	-4.45	-2.38	-0.37
power reduc.	*0.21*	*0.27*	*0.27*	*0.21*	*0.20*	*0.22*	*0.24*	*0.22*	*0.28*	*0.31*
MMSE/fixed	-17.88	-15.95	-13.87	-11.88	-9.96	-7.87	-5.88	-3.96	-1.87	0.12
MF/fixed	-17.59	-15.63	-13.58	-11.59	-9.64	-7.58	-5.60	-3.63	-1.58	0.43
Power reduc.	*0.29*	*0.32*	*0.29*	*0.29*	*0.32*	*0.29*	*0.28*	*0.33*	*0.29*	*0.31*
MMSE/adap.	-18.54	-16.55	-14.54	-12.52	-10.50	-8.55	-6.54	-4.57	-2.55	-0.53
MF/adap.	-18.05	-16.00	-14.01	-12.04	-10.10	-8.02	-6.02	-4.03	-2.05	-0.02
Power reduc.	*0.49*	*0.55*	*0.53*	*0.48*	*0.40*	*0.53*	*0.52*	*0.54*	*0.50*	*0.51*
MMSE/fixed	-17.77	-15.80	-13.74	-11.77	-9.80	-7.74	-5.77	-3.80	-1.74	0.23
MF/fixed	-17.15	-15.15	-13.20	-11.15	-9.15	-7.19	-5.12	-3.11	-1.13	0.96
Power reduc.	*0.62*	*0.65*	*0.54*	*0.62*	*0.65*	*0.55*	*0.65*	*0.69*	*0.61*	*0.73*
MMSE/adap.	-18.26	-16.28	-14.23	-12.28	-10.33	-8.30	-6.26	-4.25	-2.28	-0.25
MF/adap.	-17.73	-15.77	-13.70	-11.70	-9.68	-7.72	-5.71	-3.67	-1.62	0.35
Power reduc.	*0.53*	*0.51*	*0.53*	*0.58*	*0.65*	*0.58*	*0.55*	*0.58*	*0.66*	*0.60*
MMSE/fixed	-17.56	-15.60	-13.49	-11.55	-9.57	-7.49	-5.55	-3.57	-1.49	0.45
MF/fixed	-16.79	-14.82	-12.89	-10.78	-8.81	-6.89	-4.76	-2.77	-0.76	1.33
Power reduc.	*0.77*	*0.78*	*0.60*	*0.77*	*0.76*	*0.60*	*0.79*	*0.80*	*0.73*	*0.88*

desirable to use the MF receiver because it is simpler to implement and exhibits power consumption almost comparable to that of the MMSE receiver.

In summary, the gain of the proposed adaptive TPC over the fixed TPC is two-fold: 1) adaptive TPC offers a better tracking ability, leading to a reduced STD of the received power/SIR, and a better BER performance; and 2) the average transmit power is lowered, leading to a reduction in power consumption.

V. CONCLUSION

A multistep adaptive closed-loop power control algorithm employing either an MMSE or an MF receiver for a DS-CDMA system in the presence of Rayleigh fading is presented and evaluated. The control algorithm aims at minimizing the target power level and regulating the transmit power to closely track the variation of the fading gain. The CLPC scheme yields a relatively low standard deviation of the received power/SIR, and a relatively low bit error rate.

At the base station, a linear filter receiver is employed for despreading. With the MMSE receiver, the target power and the filter coefficients are updated iteratively. This forward loop power control algorithm is shown to be robust and converges quickly to the optimal MMSE filter coefficients, as well as minimizes the target power level. When the MF receiver is used, the filter coefficients assume the form of the signature sequence. At the mobile station, transmit power is updated with variable stepsizes, which are generated based on the power control command history and information pertaining to the Doppler effect and fading statistics.

Simulation results show that the proposed MMSE/MF iterative algorithm can converge quickly. The proposed multistep adaptive TPC exhibits a better tracking ability than the fixed stepsize TPC. The STD of the received power/SIR can be reduced significantly, leading to a better BER performance. It is shown that the improvement becomes more significant as the normalized Doppler frequency increases. In addition, adaptive TPC also leads to a reduction in average transmit power. Numerical results indicate that the tracking ability of the MMSE and MF receivers is essentially similar, except that the average transmit power is lower with the MMSE receiver but is more complex to implement. From the implementation complexity and performance tradeoff point of view, the MF receiver may be the appropriate choice in conjunction with the closed-loop power control strategy presented in the paper.

It is conjectured that the proposed adaptive stepsize algorithm can be extended to fading models which include other fading components, e.g., Rician fading with different Rice factors. The iterative update of the reference stepsize vector provides an approach to track the variations of the fading gain as a function of the Doppler frequency.

It was mentioned in the Introduction that signals sent through the dedicated control channel in IMT-2000 can be used to adaptively generate the variable stepsize to regulate the transmit power level. Thus, the proposed multistep closed-loop power control strategy can be used for third-generation and beyond wireless communication systems.

REFERENCES

[1] W. C. Y. Lee, "Overview of cellular CDMA," *IEEE Trans. Veh. Technol.*, vol. 40, pp. 291–301, May 1991.
[2] A. M. Viterbi and A. J. Viterbi, "Erlang capacity of a power controlled CDMA system," *IEEE J. Select. Areas Commun.*, vol. 11, no. 6, pp. 892–900, Aug. 1993.
[3] S. Ariyavisitakul and L. F. Chang, "Signal and interference statistics of a CDMA system with feedback power control," *IEEE Trans. Commun.*, vol. 41, pp. 1636–1634, Nov. 1993.

[4] J. W. Mark and W. Zhuang, *Wireless Communications and Networking*. Englewood Cliffs, NJ: Prentice-Hall, 2003.

[5] J. W. Mark and S. Zhu, "Wideband CDMA in third generation cellular communication systems," in *Encyclopedia of Telecommunications*, J. Proakis, Ed. New York: Wiley, 2002, vol. 5, pp. 2872–2883.

[6] A. Chockalingam, P. Dietrich, L. B. Milstein, and R. R. Rao, "Performance of closed-loop power control in DS-CDMA cellular systems," *IEEE Trans. Veh. Technol.*, vol. 47, pp. 774–789, Aug. 1998.

[7] I. Saarinen, A. Mammela, P. Jarvensiuv, and K. Ruotsalainen, "Power control in feedback communications over a fading channel," *IEEE Trans. Veh. Technol.*, vol. 50, pp. 1231–1239, Sept. 2001.

[8] F. Adachi, M. Sawahashi, and H. Suda, "Wideband DS-CDMA for next-generation mobile communications systems," *IEEE Commun. Mag.*, vol. 36, pp. 56–69, Sept. 1998.

[9] S. Nourizadeh, P. Taaghol, and R. Tafazolli, "A novel closed loop power control for UMTS," *3G Mobile Commun. Technol.*, pp. 56–59, 2000.

[10] C. C. Lee and R. Steele, "Closed-loop power control in CDMA systems," *Proc. IEEE*, vol. 143, no. 4, pp. 231–239, Aug. 1996.

[11] J. W. Mark and S. Zhu, "Power control and rate allocation in multirate wideband CDMA systems," in *Proc. IEEE Wireless Communications Networking Conf.*, 2000, pp. 168–172.

[12] J. T. Wu and E. Geraniotis, "Power control in multi-media CDMA networks," in *Proc. IEEE Vehicular Technology Conf.*, 1995, pp. 789–793.

[13] L. C. Yun and D. G. Messerschmitt, "Power control for variable QoS on a CDMA channel," in *Proc. IEEE Military Communications Conf.*, Oct. 1994, pp. 178–182.

[14] U. Madhow and M. L. Honig, "MMSE interference suppresion for direct-sequence spread-spectrum CDMA," *IEEE Trans. Commun.*, vol. 42, no. 12, pp. 3178–3188, Dec. 1994.

[15] M. L. Honig, U. Madhow, and S. Verdú, "Blind adaptive multiuser detection," *IEEE Trans. Inform. Theory*, vol. 41, no. 4, pp. 944–960, 1995.

[16] S. Ulukus and R. D. Yates, "Adaptive power control with MMSE multiuser detectors," in *Proc. IEEE Int. Conf. Communications*, 1997, pp. 361–365.

[17] M. K. Varanasi and B. Aazhang, "Multistage detection in asynchronous code-division multiple-access communications," *IEEE Trans. Commun.*, vol. 38, pp. 509–519, Apr. 1990.

[18] P. S. Kumar and J. Holtzman, "Power control for a spread spectrum system with multiuser receivers," in *Proc. IEEE Int. Symp. Personal, Indoor, and Mobile Radio Communications*, 1995, pp. 955–959.

[19] J. Zhang and E. K. P. Chong, "CDMA systems in fading channels: Admissibility, network capacity, and power control," *IEEE Trans. Inform. Theory*, vol. 46, pp. 962–981, May 2000.

[20] R. D. Yates, "A framework for uplink power control in cellular radio systems," *IEEE J. Select. Areas Commun.*, vol. 13, pp. 1341–1347, Sept. 1995.

[21] W. C. Jakes, *Microwave Mobile Communications*. New York: Wiley, 1993.

[22] L. Zhao and J. W. Mark, "Mobile speed estimation based on average fade slope duration," *IEEE Trans. Commun.*, to be published.

[23] *Japan's Proposal for Candidate Radio Transmission Technology on IMT-2000: W-CDMA*, June 1998.

Lian Zhao (S'99–M'03) received the Ph.D. degree in electrical and computer engineering from the University of Waterloo, Waterloo, ON, Canada, in 2002.

From October 2002 to July 2003, she was a Postdoctoral Fellow with the Centre for Wireless Communications, University of Waterloo. She joined the Electrical and Computer Engineering Department, Ryerson University, Toronto, ON, Canada, as an Assistant Professor in August 2003. Her research interests are in the areas of wireless communications, radio resource management for WCDMA-based communication systems, error control, power control, channel modeling, and wireless networks.

Jon W. Mark (M'62–SM'80–F'88–LF'03) received the B.A.Sc. degree from the University of Toronto, ON, Canada, in 1962 and the M.Eng. and Ph.D. degrees from McMaster University, Hamilton, ON, Canada, in 1968 and 1970, respectively, all in electrical engineering.

From 1962 to 1970, he was an Engineer and then Senior Engineer with Canadian Westinghouse Co. Ltd., Hamilton. In 1970 he joined the Department of Electrical and Computer Engineering, University of Waterloo, ON, where he is currently a Distinguished Professor Emeritus. He was Department Chairman during 1984–1990. In 1996 he established the Centre for Wireless Communications at the University of Waterloo and is currently its Founding Director. He was on sabbatical leave at the IBM T. J. Watson Research Center, Yorktown Heights, NY, as a Visiting Research Scientist (1976–1977); AT&T Bell Laboratories, Murray Hill, NJ, as a Resident Consultant (1982–1983); Laboratoire MASI, Université Pierre et Marie Curie, Paris, France, as an Invited Professor (1990–1991); and the Department of Electrical Engineering, National University of Singapore, as a Visiting Professor (1994–1995). He previously worked in the areas of adaptive equalization, spread-spectrum communications, and antijamming secure communication over satellites. His current research interests are in broadband and wireless communication networks, including network architecture, routing, and control, and resource and mobility management in wireless and hybrid wireless/wireline communication networks.

Dr. Mark was an Editor of the IEEE TRANSACTIONS ON COMMUNICATIONS (1983–1990); the Technical Program Chairman of INFOCOM'89; a a member of the Inter-Society Steering Committee of the IEEE/ACM TRANSACTIONS ON NETWORKING (1992–2003); an Editor of *Wireless Networks* (1993-2004); and an Associate Editor of *Telecommunication Systems* (1994–2004).